European Journal of Radiology 121 (2019) 108688

Contents lists available at ScienceDirect

European Journal of Radiology

journal homepage: www.elsevier.com/locate/ejrad

Research article

# Baseline clinical and imaging predictors of treatment response and overall survival of patients with metastatic melanoma undergoing immunotherapy

Amadeus Schraag[a], Bernhard Klumpp[b], Saif Afat[a], Sergios Gatidis[a], Konstantin Nikolaou[a], Thomas K. Eigentler[b], Ahmed E. Othman[a,*]

[a] Department for Diagnostic and Interventional Radiology, Eberhard Karls University Tuebingen, University Hospital Tuebingen, 72076, Tübingen, Germany
[b] Division of Dermatooncology, Department of Dermatology, Eberhard Karls University Tuebingen, University Hospital Tuebingen, Liebermeisterstr. 25, 72074, Tuebingen, Germany

ARTICLE INFO

*Keywords:*
Melanoma
Immunotherapy
Survival analysis
Tomography
Spiral computed

ABSTRACT

*Purpose:* We aimed to identify predictive clinical and CT imaging biomarkers and assess their predictive capacity regarding overall survival (OS) and treatment response in patients with metastatic melanoma undergoing immunotherapy.

*Methods:* The local institutional ethics committee approved this retrospective study and waived informed patient consent. 103 patients with immunotherapy for metastatic melanoma were randomly divided into training (n = 69) and validation cohort (n = 34). Baseline tumor markers (LDH, S100B), baseline CT imaging biomarkers (tumor burden, Choi density) and CT texture parameters (Entropy, Kurtosis, Skewness, uniformity, MPP, UPP) of the largest target lesion were extracted. To identify treatment response predictors, binary logistic regression analysis was performed in the training cohort and tested in the validation cohort. For OS, Cox regression and Kaplan Maier analyses were performed in the training cohort. Bivariate and multivariate models were established. Goodness of fit was assessed with Harrell's C-index. Potential predictors were tested in the validation cohort also using Cox-regression and Kaplan-Meier analyses.

*Results:* Baseline S100B (Hazard ratio(HR) = 2.543, p0.018), tumor burden (HR = 1.657, p = 0.002) and Kurtosis (HR = 2.484, $p < 0.001$) were independent predictors of OS and were confirmed in the validation cohort ($p < 0.048$). Tumor burden and Kurtosis showed incremental predictive capacity allowing a good predictive model when combined with baseline S100B levels (C-index = 0.720). Only S100B was predictive of treatment response (OR ≤ 0.630, p ≤ 0.022). Imaging biomarkers did not predict treatment response.

*Conclusion:* We identified easily obtainable baseline clinical (S100B) and CT predictors (tumor burden and Kurtosis) of OS in patients with metastatic melanoma undergoing immunotherapy. However, imaging predictors did not predict treatment response.

## 1. Introduction

Melanoma is the most common cancer in young adults with rising incidence, especially in western countries [1]. Patients with metastatic melanoma have poor prognosis [2]. Advances in systemic, especially immunotherapy, led to a remarkable increase of survival rates in metastatic melanoma patients [3,4]. However, more than half of the patients do not respond to immunotherapy and have worse prognosis than responders [5]. Therefore, identification of baseline response and survival predictors in these patients is crucial and could help stratifying patients for the right therapy choice. To date, only few clinical baseline survival predictors have been identified in metastatic melanoma patients undergoing immunotherapy, for example serum Lactate dehydrogenase (LDH) and S100B [6]. In these patients, routine CT imaging is performed prior to therapy at baseline and during immunotherapy to assess treatment response [7]. The availability of baseline imaging in these patients allows for assessment of the CT imaging biomarkers as outcome predictors. Standard imaging biomarkers such as tumor burden and CT density of the tumor metastases (i.e. Choi density) [8] as well as texture features [9] can be extracted from baseline CT images.

*Abbreviations:* HR, hazard ratio; LDH, lactate dehydrogenase; MPP, mean of positive pixels; OR, odds ratio; OS, overall survival; ROI, regions of interest; UPP, uniformity of positive pixel distribution

* Corresponding author at: Department of Diagnostic and Interventional Radiology, University Hospital Tuebingen, Hoppe-Seyler-Straße 3, 72076 Tuebingen Germany.
*E-mail address:* ahmed.e.othman@googlemail.com (A.E. Othman).

https://doi.org/10.1016/j.ejrad.2019.108688
Received 8 May 2019; Received in revised form 23 August 2019; Accepted 17 September 2019

We hypothesize that baseline imaging biomarkers have an additional predictive capacity to known clinical predictors for patient survival and treatment response. Therefore, we aimed to identify predictive standard imaging biomarkers as well as CT texture features and assess their predictive capacity alone and in combination with significant clinical predictors with regards to overall survival (OS) and treatment response in patients with metastatic melanoma undergoing immunotherapy

## 2. Methods and materials

The institutional ethics committee of the university hospital approved this retrospective study and waived informed patient consent.

### 2.1. Study population

We searched for eligible patients in our prospectively maintained melanoma registry at our melanoma center during a ten-year period between 06/2006 - 06/2016. Patients were eligible if they met the following inclusion criteria: i) metastatic melanoma, ii) systemic therapy with immunotherapy (Anti-PD1, CTLA 4 or a combination of both), iii) available baseline demographics and tumor markers (LDH and S100B) and iv) available standard contrast enhanced portal venous phase whole-body CT prior to therapy. Patients were excluded if time between baseline imaging and clinical data exceeded two months.

After exclusion of ineligible patients, the final sample was randomly assigned to a training and a validation cohort with a ratio of 2:1 (training cohort n = 69, validation cohort n = 34). A Flowchart of the inclusion process is presented in Fig. 1.

### 2.2. Imaging protocol and image quality analysis

All patients underwent contrast enhanced standard dose whole-body CT staging comprising the region between skull base and groin.

Image quality was assessed prior to further image analysis, since texture parameters may be affected by image quality and image noise. Overall image quality and diagnostic confidence of CT images were assessed qualitatively by two readers (AO and SA) with six years and four years of experience in oncologic imaging, respectively. Image quality analysis was performed on a 4-point Likert-scale (1 = poor image quality/ low diagnostic confidence, 2 = moderate image quality/ moderate diagnostic confidence, 3 = good image quality/high diagnostic confidence, 4 = excellent image quality/very high diagnostic confidence).

Furthermore, quantitative image noise analysis was performed. Therefore, two regions of interest (ROI) were drawn in the subcutaneous fat at the level of L1 by one reader (SA). Image noise was defined as the standard deviation of the ROIs.

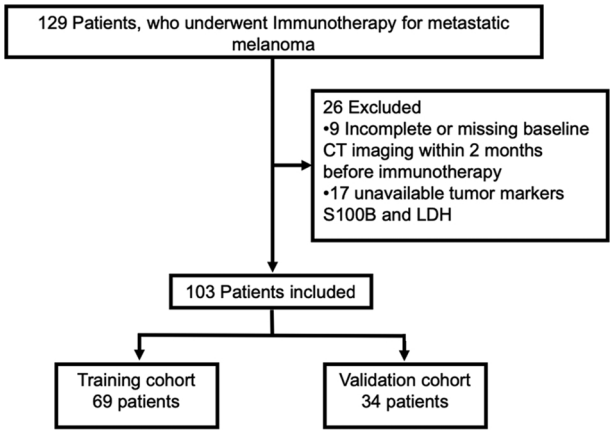


**Fig. 1.** STARD flowchart of patient inclusion and assignment to training and validation Cohort.

**Table 1**
Baseline demographics and patient characteristics of training and validation cohorts.

| | | Training cohort (n = 69) | Validation cohort (n = 34) | P Value |
|---|---|---|---|---|
| Sex | M | 42 | 20 | 1.000 |
| | F | 27 | 14 | |
| Median age (y) | | 57 (26-82) | 42.5 (30-74) | 0.024 |
| LDH | Normal | 47 | 19 | 0.159 |
| | elevated | 22 | 15 | |
| S100B | Normal | 29 | 12 | 0.331 |
| | Elevated | 40 | 22 | |
| Immunotherapy | CTLA-4 | 55 | 30 | 0.158 |
| | PD1 | 13 | 3 | |
| | Blinded | 1 | 1 | |
| Survival and response | | | | |
| Response (RECIST1.1) | CR | 1 | 3 | 0.805 |
| | PR | 13 | 3 | |
| | SD | 13 | 9 | |
| | PD | 42 | 19 | |
| Overall survival (d) | | 438 (52-3226) | 476 (77-1831) | 0.643 |

**Table 2**
Baseline standard imaging and texture parameter of training and validation cohorts.

| Parameter | Training cohort | Validation cohort | p value |
|---|---|---|---|
| Tumor burden (mm) | 73.65 ± 66.24 | 92.33 ± 77.24 | 0.110 |
| Choi density (HU) | 53.23 ± 24.39 | 54.34 ± 24.04 | 0.305 |
| Entropy | 6.07 ± 0.42 | 6.21 ± 0.53 | 0.147 |
| Kurtosis | 7.87 ± 15.37 | 7.18 ± 9.38 | 0.994 |
| Skewness | −0.65 ± 1.58 | −0.98 ± 1.36 | 0.045* |
| Uniformity | 0.018 ± 0.005 | 0.017 ± 0.006 | 0.387 |
| MPP (HU) | 58.77 ± 32.43 | 57.20 ± 23.43 | 0.219 |
| UPP | 0.017 ± 0.006 | 0.016 ± 0.006 | 0.097 |

* significant.

### 2.3. Image analysis

Image analysis was performed using a structured reporting platform (Mint lesion™ 3.0, Mint Medical, Dossenheim, Germany). All images were analyzed by one specialist reader (BK) with 12 years of experience in oncologic imaging. The reader defined the target lesions according to RECIST 1.1 [10]. The tumor burden was defined as sum of diameters of the target lesions given in mm. Furthermore, the reader identified the largest target lesion on the baseline CT and extracted Choi density as well as first order texture parameters using the above mentioned structured reporting software (Mint lesion™). To this end, the reader selected the axial slice with the largest area of the respective lesion then placed a free-hand ROI containing the entire metastasis. The parameters Choi density, Entropy, Kurtosis, Skewness, Uniformity, Mean of positive pixels (MPP) and uniformity of positive pixel distribution (UPP) were extracted.

The reader also assessed treatment response according to RECIST 1.1 [10].

### 2.4. End points

The aim of this study was to identify imaging and clinical predictors for OS and treatment response.

The primary endpoints are the following:

1 OS defined as the time between initiation of immunotherapy and death.
2 Treatment response at first follow-up imaging (12 weeks after initial therapy) according to RECIST 1.1 [10]. Prior to statistical analysis, treatment response was dichotomized as follows: Complete

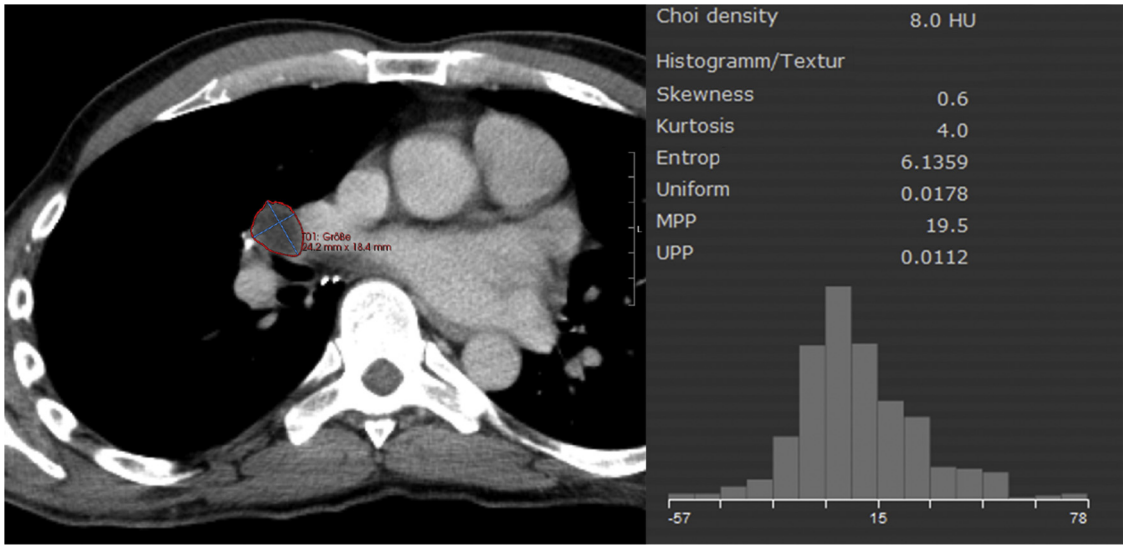


**Fig. 2.** Baseline CT images 18 days prior to treatment in a 50-year-old male patient with metastatic melanoma; segmentation of the largest metastasis (hilar lymph node) with corresponding Choi density and texture features. The overall survival of the patient was 952 days.

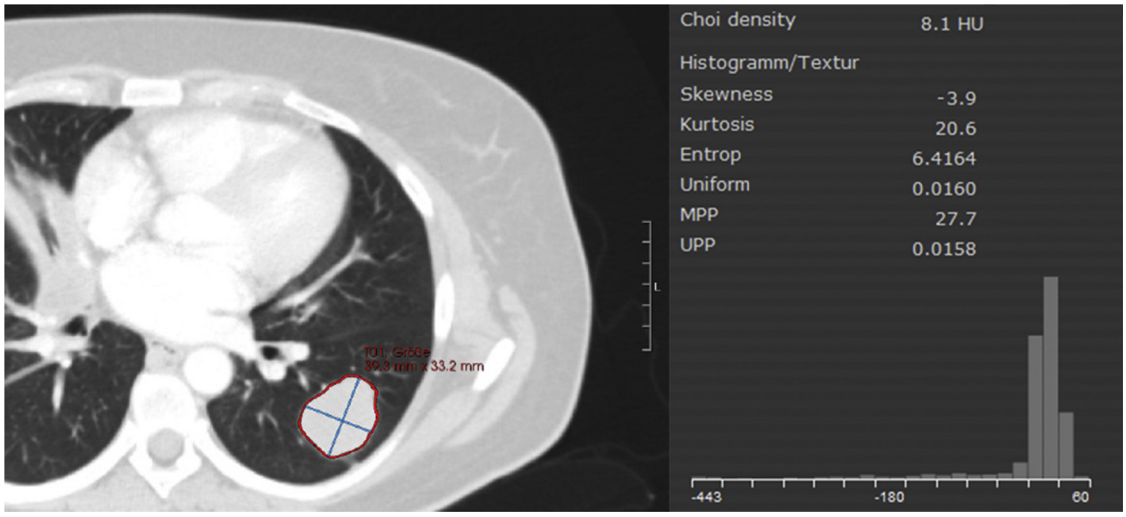


**Fig. 3.** Baseline CT images 18 days prior to treatment in a 43-year-old female patient with metastatic melanoma; segmentation of the largest metastasis (pulmonary metastasis) with corresponding Choi density and texture features. The overall survival of the patient was 145 days.

remission (CR), partial response (PR) and stable disease (SD) were considered as treatment response, whereas progressive disease (PD) was considered as lack of response.

### 2.5. Statistical analysis

The clinical predictors LDH and S100B and the standard imaging predictors tumor burden and Choi density as well as the texture parameters Entropy, Kurtosis, Skewness, Uniformity, MPP and UPP were used as predictors for OS and treatment response. Prior to comparative analyses, all variables were assessed for normal distribution using the Shapiro-Wilk test. The tumor markers lactate dehydrogenase (LDH) and S100B were categorized into normal and elevated levels using the clinically established cut-off values 250 U/l for LDH [11] and 0.15 µg/l for S100B [12]. The imaging predictors and texture parameters were normalized to mean 0 and standard deviation 1 (Z-score). For comparison of training and validation cohorts, variables were assessed using $X^2$, Mann-Whitney U test or *t*-test as appropriate. Inter-rater agreement for image quality analysis was assessed using Cohen's Kappa.

#### 2.5.1. Training cohort

The variables LDH, S100B, Tumor burden, Choi density and texture parameters were further assessed as predictors for treatment response and OS.

For prediction of OS, univariate Cox regression was performed for each clinical variables (LDH and S100B), standard imaging variables (tumor burden and Choi density) and texture variables. All significant predictors in the univariate analyses were then analyzed using multivariable cox regression analysis. Significant predictors in multivariable analyses were then used to build four different predictive models: i) clinical and standard imaging predictors, ii) clinical and texture predictors, iii) standard imaging predictors and texture predictors and iv) clinical predictors, standard imaging predictors and texture predictors. The concordance of each model was assessed using Harrell`s C-index. Harrell`s C-index was interpreted as follows: < 0.7 = poor model, 0.7-0.8 = good model, > 0.8 = strong model. Furthermore, Kaplan Maier analysis was performed for predictors, which were significant in multivariable analysis. Therefore, an optimal threshold for each significant standard imaging and texture parameter was identified by using a multiparametric log-rank test. A p-value of ≤ 0.05 was considered

**Table 3**
Univariate and multivariate Cox-regression analysis in the training cohort for survival prediction.

| | | | |
|---|---|---|---|
| Univariate Cox-regression | | | |
| Predictor | Hazard ratio | 95%-CI | p |
| LDH | 0.930 | 0.470 – 1.840 | 0.836 |
| S100B | 3.376 | 1.637 – 6.962 | 0.001* |
| Tumor burden | 1.837 | 1.353 – 2.466 | < .001* |
| Choi density | 0.790 | 0.500 – 1.247 | 0.301 |
| Entropy | 1.173 | 0.863 – 1.592 | 0.308 |
| Kurtosis | 1.612 | 1.259 – 2.062 | < 0.001* |
| Skewness | 0.814 | 0.531 - 1.246 | 0.343 |
| Uniformity | 0.936 | 0.679 – 1.291 | 0.689 |
| MPP | 0.951 | 0.714 - 1.267 | 0.732 |
| UPP | 0.979 | 0.728 – 1.316 | 0.887 |
| Multivariate Cox-regression | | | |
| Clinical predictors and standard imaging predictors | | | |
| S100B | 2.702 | 1.149 – 2.163 | 0.010* |
| Tumor burden | 1.577 | 1.149 – 2.163 | 0.005* |
| Clinical and Texture predictors | | | |
| S100B | 3.268 | 1.575 – 6.781 | 0.001* |
| Kurtosis | 1.538 | 1.204 – 1.963 | 0.001* |
| Standard imaging and Texture predictors | | | |
| Tumor burden | 1.912 | 1.409 – 2.594 | < 0.001* |
| Kurtosis | 1.686 | 1.315 – 2.162 | < 0.001* |
| Clinical predictors, standard imaging predictors and texture predictors | | | |
| S100B | 2.543 | 1.177 – 5.494 | 0.018* |
| Tumor burden | 1.657 | 1.201 – 2.291 | 0.002* |
| Kurtosis | 1.611 | 1.256 – 2.065 | < 0.001* |

* significant.

significant. To account for multiple comparisons, false discovery rate (FDR) correction using the Benjamini-Hochberg method was performed with a false discovery rate at 0.05.

#### 2.5.2. Validation cohort

Significant predictors were assessed using univariate cox-regression as well as Kaplan Maier and non-parametric log-rank test using the cut-off values derived from the training cohort. To account for multiple comparisons, FDR correction using the Benjamini-Hochberg method was performed with a false discovery rate at 0.05. Furthermore, Harrell`s C-index was calculated for the same four models as in the training cohort in order to validate the predictive capacity of each model.

## 3. Results

### 3.1. Patient characteristics

Patient demographics and comparative results of training and validation cohort are provided in Table 1. Eighty-five patients received the CTLA-4 inhibitor Ipilimumab (training cohort n = 55, validation cohort n = 30). Eight patients received the PD-1-inhibitor Nivolumab (training cohort n = 7, validation cohort n = 1) and eight patients received the PD-1-inhibitor Pembrolizumab (training cohort n = 6, validation cohort n = 2). Two patients (one patient in the training cohort and one patient in the validation cohort), who participated in a clinical trial were still blinded regarding therapy arm [13]. There were no significant differences regarding type of immunotherapy between the two cohorts (p = 0.158). We found no significant differences between the two cohorts regarding sex, tumor markers (LDH and S100B), treatment response or OS. However, both cohorts showed significant differences regarding patient age (median age: 57 y in training cohort, 42.5 y in validation cohort, p = 0.024). Median time between baseline imaging and initiation of immunotherapy was 17 days (0–56 days) in the training cohort and 18 days (0–63 days) in the validation cohort without significant differences between both cohorts (p = 0.415). In the training cohort, OS was censored in 30 patient, in the validation cohort, OS was censored in 12 patient.

### 3.2. Image quality analysis

Overall Image quality was sufficient in both cohorts without significant differences (training cohort: median = 4, range 3–4, validation cohort: median = 4, range 3–4, p = 0.186) and diagnostic confidence was very high in all patients without significant cohort differences (training and validation cohort: median = 4, range 4-4, p = 1.00) for both readers with a high inter-rater agreement (Kappa > 0.718). None of the CT datasets revealed poor image quality or low diagnostic confidence.

Image noise was 9.99 ± 2.73 HU in the training cohort and 10.07 ± 2.24 HU in the validation cohort without significant differences between both cohorts (p = 0.734).

### 3.3. Image analysis

Results of image analysis including results of texture analysis are provided in Table 2 and patient examples are given in Figs. 2 and 3. The texture parameter skewness showed significant differences between both cohorts (p = 0.045). No significant differences were detected between training and validation cohort regarding all other standard imaging parameters (tumor burden and Choi density) or texture parameters, see Table 2.

### 3.4. Univariate and multivariate analysis for prediction of OS in the training cohort

The results of univariate Cox regression in the training cohort are provided in Table 3. In univariate analyses, baseline S100B (normal vs. elevated, HR = 3.376, 95%-CI 1.637–6.962, p = 0.001), tumor burden (HR = 1.837, 95%-CI 1.353–2.466, p < 0.001) and Kurtosis

**Table 4**
Log-rank test of significant predictors in training and validation cohort.

| Training Cohort | | | | | |
|---|---|---|---|---|---|
| Predictor | Value | Threshold | Median OS (d) | | p (Benjamini-Hochberg) |
| | | | above threshold | below threshold | |
| S100B | Normal or elevated | – | 231 | > 3226* | 0.001 |
| Tumor burden (mm) | 73.65 ± 66.24 mm | 103 mm | 128 | 1230 | < 0.001** |
| Kurtosis | 7.87 ± 15.37 | 7.85 | 231 | 785 | 0.032** |
| Validation Cohort | | | | | |
| S100B | Normal or elevated | – | 270 | > 1352* | 0.015** |
| Tumor burden (mm) | 92.33 ± 77.24 mm | 103 | 238 | 1831 | 0.002** |
| Kurtosis | 7.18 ± 9.38 | 7.85 | 145 | 1050 | 0.002** |

* median not reached.
** significant.

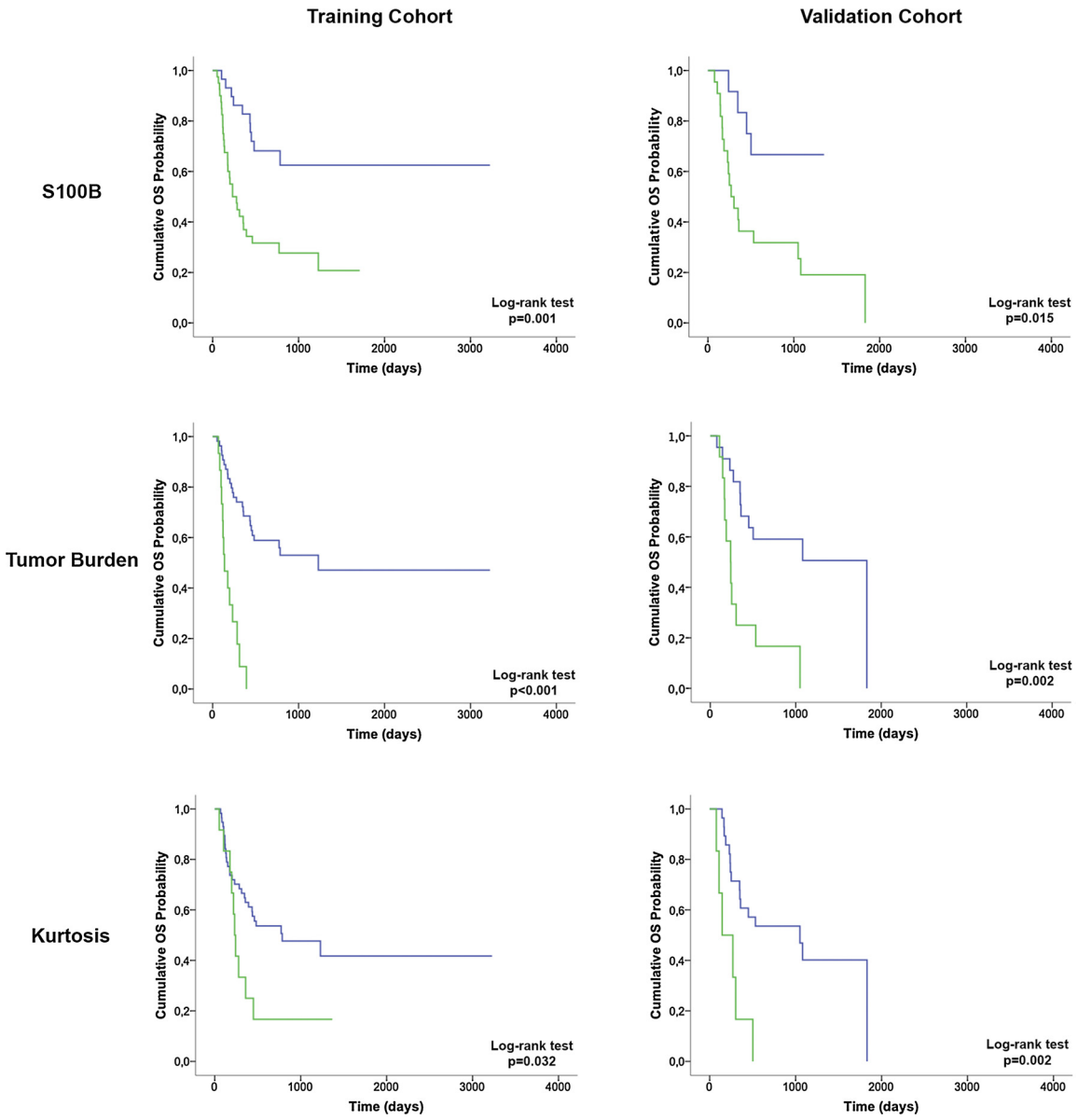


**Fig. 4.** Kaplan-Meier survival analysis in training and validation cohort. Green curves represent patients with values above threshold, blue curves represent patients with values below threshold.

**Table 5**
C-index as a Goodness of fit measure of the three models in training and validation cohort.

| Predictive model | C-index | |
|---|---|---|
| | Training cohort | Validation cohort |
| Clinical model (S100B) | 0.656 | 0.645 |
| Standard imaging model (Tumor burden) | 0.623 | 0.674 |
| Texture model (Kurtosis) | 0.533 | 0.633 |
| Clinical and standard imaging model | 0.687 | 0.710 |
| Clinical and texture model | 0.676 | 0.716 |
| Standard imaging and texture model | 0.664 | 0.695 |
| Clinical, standard imaging and texture model | 0.720 | 0.716 |

(HR = 1.612, 95%-CI 1.259–2.062, p < 0.001) were significantly associated with OS, see Table 3.

These predictors maintained their prognostic significance in multivariable analyses (S100B: HR = 2.543, 95%-CI 1.177–5.494, p = 0.018; Tumor burden: HR = 1.657, 95%-CI 1.201–2.291, p = 0.002; Kurtosis: HR = 1.611, 95%-CI 1.256–2.065, p < 0.001), see Table 3.

After applying FDR correction using the Benjamini-Hochberg method, univariate Kaplan-Meier analysis also revealed significant association with OS for S100B (p = 0.001), tumor burden (< 0.001, cut-off 103 mm) and Kurtosis (p = 0.032, cut-off 7.85), see Table 4 and Fig. 4.

The C-index, was highest for the model including all three predictors and reached a good predictive capacity (C-index = 0.720), see Table 5.

### 3.5. Validation of predictors in the validation cohort

The predictors S100B (normal vs. elevated, HR = 3.553, 95%-CI

1.190–10.610, p = 0.023), tumor burden (HR = 1.918, 95%-CI 1.287–2.858, p = 0.001) and Kurtosis (HR = 1.614, 95%-CI 1.004–2.594, p = 0.048) maintained their predictive capacity in univariate Cox regression analysis in the validation cohort. The above-mentioned predictors also revealed significant association with OS in Kaplan-Meier analysis with the same cut-offs which were derived from the training cohort (S100B: p = 0.015; Tumor burden: p = 0.002, cut-off 103 mm; Kurtosis: p = 0.002, cut-off 7.85), see Table 4 and Fig. 4.

Similar to the training cohort, the C-index was high for the model including all three predictors reaching a good predictive capacity (C-index = 0.716), see Table 5.

### 3.6. Analysis for prediction of treatment response

S100B was a significant predictor of treatment response (normal vs. elevated, Odds ratio, OR = 0.630, 95%-CI = 0.112 – 0.845, p = 0.22). None of the analyzed clinical or imaging parameters significantly predicted treatment response at first follow-up (p ≥ 0.372).

The predictive capacity of S100B was validation in the validation cohort (OR = 0.125, 95%-CI = 0.025 – 0.624, p = 0.011).

## 4. Discussion

In this study, we could identify independent baseline clinical and imaging predictors of OS in metastatic melanoma patients undergoing immunotherapy. As clinical baseline predictor, elevated S100B levels had a hazard ratio of 2.543 in multivariable analysis. S100B is a low molecular calcium binding protein and is known to be a useful predictive marker in melanoma patients [6] with a superior predictive capacity in comparison with LDH [14].

Along with S100B, tumor burden at baseline imaging (expressed as the sum of the diameters of target lesions according to RECIST 1.1) had an independent predictive capacity for OS in these patients with a hazard ratio of 1.657 in multivariable analysis. This finding is of particular interest, since this biomarker is easily and routinely obtained in these patients, who are usually participating in clinical therapy trials.

Furthermore, Kurtosis of the largest target lesion was identified as an independent texture predictor for OS with a hazard ratio of 1.611. Kurtosis is a first order histogram texture feature expressing the pixel peakedness or pointiness of the pixels in the included region of interest [9].

The three predictors also revealed significant association with OS in Kaplan-Meier analysis. The two identified imaging predictors had an additive predictive capacity to the clinical predictor S100B and the combination of the three clinical and imaging biomarkers increased the predictive capacity of the model with a C-index of 0.720, which indicates a good model. Regarding treatment response, we could not identify any predictive baseline clinical or imaging biomarkers in our cohort of metastatic melanoma patients prior to immunotherapy.

The three predictors could be confirmed in the validation cohort showing significant results in Cox regression and significant association with OS in Kaplan-Meier analysis when applying the thresholds, which were extracted from the training cohort.

Few studies have extracted imaging biomarkers for survival prediction in melanoma patients. Gray et al. (2014) for instance demonstrated an independent predictive capacity of MASS criteria from first follow-up CT images after initiation of antiangiogenic therapy in patients with metastatic melanoma [15]. The same group demonstrated the predictive value of CT texture analysis for survival of patients with metastatic melanoma and stable disease after initiation of anti-angiogenic therapy [16]. In this particular study, the authors reported predictive properties of the change of texture features in these patients of the target lesions from baseline to first post-therapy CT imaging. The above-mentioned studies are of high relevance, however, the therapy of patients included in their analyses is not the therapy of choice for metastatic melanoma. Furthermore, the authors identified imaging biomarkers at first follow-up after therapy initiation and not at baseline.

To our knowledge, the present study is the first to investigate imaging biomarkers solely extracted from baseline CT imaging in a representative patient cohort with metastatic melanoma undergoing immunotherapy, which is the therapy of choice at present.

However, this study has limitations. The retrospective design inherits the risk of selection bias. Nonetheless, we were able to identify all eligible patients from our prospectively maintained registry of our melanoma center. The CT images were acquired in different scanners, which may cause variability in texture parameters. However, image quality of the CT data as well as image noise did not differ significantly between groups. The sample size is relatively small to assess a high number of predictors, but a sample size of 103 patients was considered sufficient for multivariable analysis applying the three significant biomarkers. A slight but difference was detected for the texture parameter skewness between training cohort and validation cohort, which can be attributed to sample size of both cohorts. We did not include higher order radiomic features or machine learning features in this study. Further studies are needed to assess the potential predictive value of these quantitative features. Finally, the included patients received different immunotherapy agents (CTLA-4 and PD-1 inhibitors). Since these agents have similar mechanisms, the inclusion of both therapy types was considered appropriate to allow for a sufficient sample size.

Before clinical use of the presented predictive model, a prospective validation of our findings is needed.

To conclude, we identified independent baseline clinical (S100B) and imaging (tumor burden and Kurtosis) in patients with metastatic melanoma undergoing immunotherapy, which when used combined have a good predictive capacity for patient survival.

## Declaration of Competing Interest

None.

## References

[1] C. Garbe, U. Leiter, Melanoma epidemiology and trends, Clin. Dermatol. 27 (1) (2009) 3–9.
[2] J. Manola, M. Atkins, J. Ibrahim, J. Kirkwood, Prognostic factors in metastatic melanoma: a pooled analysis of Eastern Cooperative Oncology Group trials, J. Clin. Oncol. 18 (22) (2000) 3782–3793.
[3] F.S. Hodi, S.J. O'Day, D.F. McDermott, R.W. Weber, J.A. Sosman, J.B. Haanen, R. Gonzalez, C. Robert, D. Schadendorf, J.C. Hassel, W. Akerley, A.J. van den Eertwegh, J. Lutzky, P. Lorigan, J.M. Vaubel, G.P. Linette, D. Hogg, C.H. Ottensmeier, C. Lebbe, C. Peschel, I. Quirt, J.I. Clark, J.D. Wolchok, J.S. Weber, J. Tian, M.J. Yellin, G.M. Nichol, A. Hoos, W.J. Urba, Improved survival with ipilimumab in patients with metastatic melanoma, N. Engl. J. Med. 363 (8) (2010) 711–723.
[4] D. Schadendorf, F.S. Hodi, C. Robert, J.S. Weber, K. Margolin, O. Hamid, D. Patt, T.T. Chen, D.M. Berman, J.D. Wolchok, Pooled analysis of long-term survival data from phase II and phase III trials of Ipilimumab in unresectable or metastatic melanoma, J. Clin. Oncol. 33 (17) (2015) 1889–1894.
[5] I. Lugowska, P. Teterycz, P. Rutkowski, Immunotherapy of melanoma, Contemp. Oncol. 22 (1A) (2018) 61–67.
[6] N.B. Wagner, A. Forschner, U. Leiter, C. Garbe, T.K. Eigentler, S100B and LDH as early prognostic markers for response and overall survival in melanoma patients treated with anti-PD-1 or combined anti-PD-1 plus anti-CTLA-4 antibodies, Br. J. Cancer 119 (3) (2018) 339.
[7] A. Pflugfelder, C. Kochs, A. Blum, M. Capellaro, C. Czeschik, T. Dettenborn, D. Dill, E. Dippel, T. Eigentler, P. Feyer, Malignes melanom S3-Leitlinie "Diagnostik, therapie und nachsorge des melanoms", JDDG: Journal der Deutschen Dermatologischen Gesellschaft 11 (s6) (2013) 1–126.
[8] H. Choi, C. Charnsangavej, S.C. Faria, H.A. Macapinlac, M.A. Burgess, S.R. Patel, L.L. Chen, D.A. Podoloff, R.S. Benjamin, Correlation of computed tomography and positron emission tomography in patients with metastatic gastrointestinal stromal tumor treated at a single institution with imatinib mesylate: proposal of new computed tomography response criteria, J. Clin. Oncol. 25 (13) (2007) 1753–1759.
[9] M.G. Lubner, A.D. Smith, K. Sandrasegaran, D.V. Sahani, P.J. Pickhardt, CT texture analysis: definitions, applications, biologic correlates, and challenges, radiographics : a review publication of the radiological society of north america, Inc 37 (5) (2017) 1483–1503.
[10] E.A. Eisenhauer, P. Therasse, J. Bogaerts, L.H. Schwartz, D. Sargent, R. Ford, J. Dancey, S. Arbuck, S. Gwyther, M. Mooney, L. Rubinstein, L. Shankar, L. Dodd,

R. Kaplan, D. Lacombe, J. Verweij, New response evaluation criteria in solid tumours: revised RECIST guideline (version 1.1), Eur. J. Cancer 45 (2) (2009) 228–247.
[11] F. Petrelli, M. Cabiddu, A. Coinu, K. Borgonovo, M. Ghilardi, V. Lonati, S. Barni, Prognostic role of lactate dehydrogenase in solid tumors: a systematic review and meta-analysis of 76 studies, Acta oncologica 54 (7) (2015) 961–970.
[12] A.A. Tarhini, J. Stuckert, S. Lee, C. Sander, J.M. Kirkwood, Prognostic significance of serum S100B protein in high-risk surgically resected melanoma patients participating in Intergroup Trial ECOG 1694, J. Clin. Oncol. 27 (1) (2009) 38–44.
[13] J. Larkin, V. Chiarion-Sileni, R. Gonzalez, J.J. Grob, C.L. Cowey, C.D. Lao, D. Schadendorf, R. Dummer, M. Smylie, P. Rutkowski, P.F. Ferrucci, A. Hill, J. Wagstaff, M.S. Carlino, J.B. Haanen, M. Maio, I. Marquez-Rodas, G.A. McArthur, P.A. Ascierto, G.V. Long, M.K. Callahan, M.A. Postow, K. Grossmann, M. Sznol, B. Dreno, L. Bastholt, A. Yang, L.M. Rollin, C. Horak, F.S. Hodi, J.D. Wolchok, Combined nivolumab and ipilimumab or monotherapy in untreated melanoma, N. Engl. J. Med. 373 (1) (2015) 23–34.
[14] F. Egberts, A. Pollex, J.H. Egberts, K.C. Kaehler, M. Weichenthal, A. Hauschild, Long-term survival analysis in metastatic melanoma: serum S100B is an independent prognostic marker and superior to LDH, Onkologie 31 (7) (2008) 380–384.
[15] M.R. Gray, S. Martin del Campo, X. Zhang, H. Zhang, F.F. Souza, W.E. Carson 3rd, A.D. Smith, Metastatic melanoma: lactate dehydrogenase levels and CT imaging findings of tumor devascularization allow accurate prediction of survival in patients treated with bevacizumab, Radiology 270 (2) (2014) 425–434.
[16] A.D. Smith, M.R. Gray, S.M. del Campo, D. Shlapak, B. Ganeshan, X. Zhang, W.E. Carson 3rd, Predicting overall survival in patients with metastatic melanoma on antiangiogenic therapy and RECIST stable disease on initial posttherapy images using CT texture analysis, AJR Am. J. Roentgenol. 205 (3) (2015) W283–93.